ResearchGate

See discussions, stats, and author profiles for this publication at: https://www.researchgate.net/publication/7542858

Intermediate filament immunohistochemistry of astroglial cells in the leopard gecko, Eublepharis macularius

ARTICLE *in* ANATOMY AND EMBRYOLOGY · DECEMBER 2005

Impact Factor: 1.39 · DOI: 10.1007/s00429-005-0049-x · Source: PubMed

CITATIONS
7

READS
24

2 AUTHORS, INCLUDING:

Valeria Franceschini
University of Bologna
71 PUBLICATIONS **520** CITATIONS

SEE PROFILE

All in-text references underlined in blue are linked to publications on ResearchGate, letting you access and read them immediately.

Available from: Valeria Franceschini
Retrieved on: 25 January 2016

Anat Embryol (2005) 210: 275–286
DOI 10.1007/s00429-005-0049-x

ORIGINAL ARTICLE

Maurizio Lazzari · Valeria Franceschini

Intermediate filament immunohistochemistry of astroglial cells in the leopard gecko, *Eublepharis macularius*

Accepted: 23 August 2005 / Published online: 13 October 2005
© Springer-Verlag 2005

Abstract The distribution of intermediate filament molecular markers, glial fibrillary acidic protein (GFAP) and vimentin, has been studied in the central nervous system (CNS) of the adult leopard gecko, *Eublepharis macularius*. This immunohistochemical study points out the presence of different astroglial cell types. The main pattern is constituted by ependymal radial glia, which have their cell bodies located in the ependymal layer throughout the brain ventricular system. Radial glia proper or radial astrocytes show their cell bodies displaced from the ependymal layer into a periependymal zone and are observed only in the spinal cord. Star-shaped astrocytes are scarce. They are detected in the ventral and lateral regions of the diencephalon and mesencephalon, in the superficial layer of the optic tectum, in the ventral medulla oblongata, and in the ventral and lateral spinal cord. In the different regions of the CNS, the staining intensity appears not to be identical even in the same cellular type. The results reported in the present study show an heterogeneous feature of the astroglial pattern in *E. macularius*.

Keywords Glial fibrillary acidic protein · Vimentin · Immunohistochemistry · Astroglial cells · Reptiles

Introduction

The cellular elements composing the radial glia have a complex shape. Their cell bodies, pear- or spindle-shaped, are arranged in the ependymal or periependymal layer where they form the ependymal or periependymal radial glia, respectively. Their long cytoplasmic processes, radially oriented to the meningeal surface and the vascular walls, terminate with end-feet that constitute the submeningeal and perivascular glial layers, respectively (Monzon-Mayor et al. 1990; Yanez et al. 1990; Elmquist et al. 1994; Lazzari et al. 1997; Lazzari and Franceschini 2001). Radial glia is considered not only the most phylogenetically primitive form of glia (Onteniente et al. 1983; Miller and Liuzzi 1986) as it is widely represented in non-mammalian vertebrates but also an ontogenetically immature type of glia since it is the first to appear during the development of mammals (Levitt and Rakic 1980).

In developing mammals, radial glia becomes progressively reduced as development proceeds, so it is virtually non-detectable in adults (Pixley and De Vellis 1984; Elmquist et al. 1994). In particular, in the cerebellum, radial glia differentiate in Bergmann glial cells (Yamada and Watanabe 2002). On the contrary, in the other vertebrates, radial glia is present throughout the entire life (Ebner and Colonnier 1975; Lazzari et al. 1997; Lazzari and Franceschini 2001).

Glial fibrillary acidic protein (GFAP), which is expressed in mature cells of the astroglial lineage (see Wasowicz et al. 1994; Wicht et al. 1994; Naujoks-Manteuffel and Meyer 1996 for reviews), represents the main component of gliofilaments included in the intermediate filament class. Therefore, this protein is widely accepted as a reliable specific molecular marker for these cells (Dahl and Bignami 1985). The GFAP shows considerable stability in its molecular and antigenic characteristics across vertebrate phylogeny as suggested by the finding that in each vertebrate group, it shows a clear cross- reactivity to the anti-mammalian GFAP antibodies (Onteniente et al. 1983; Dahl et al. 1985; Bodega et al. 1994).

Vimentin is the component of another intermediate filament type of the glial cells. This protein is expressed in immature cells of the astroglial lineage in reptiles (Monzon-Mayor et al. 1990; Yanes et al. 1990; Lazzari and Franceschini 2001) and mammals (Elmquist et al. 1994; Pulido-Caballero et al. 1994), but in teleosts and amphibians it is still found in adult glial elements (Zamora and Mutin 1988; Cardone and Roots 1990;

M. Lazzari (✉) · V. Franceschini
Department of Biology, University of Bologna,
Via Selmi 3, 40126 Bologna, Italy
E-mail: maurizio.lazzari@unibo.it
Tel.: +39-051-2094145
Fax: +39-051-2094286

Rubio et al. 1992; Lazzari et al. 1997). The cross-reaction of antibodies produced against mammalian vimentin with the corresponding protein in birds and amphibians suggests that also vimentin is highly conserved during vertebrate phylogeny (Bennett et al. 1978; Szaro and Gainer 1988; Zamora and Mutin 1988; Bodega et al. 1994).

The presence of these intermediate filament molecular markers in the different astroglial cell types, as well as the relative proportion and the regional distribution of these astrocytic subtypes in the central nervous system (CNS) of different vertebrates appear very important in ontogenetic and phylogenetic studies (Elmquist et al. 1994; Monzon-Mayor et al. 1998; Kalman and Pritz 2001; Lazzari and Franceschini 2001).

Comparative research on glial cells in the CNS of different vertebrates will bring new findings about the phylogenetic and ontogenetic relations between the different cell types included in the glial-cell lineage.

Studies on reptilian glial cells are still relatively scarce (Dahl and Bignami 1973; Onteniente et al. 1983; Kalman et al. 1994, 1997; Kalman and Pritz 2001). In particular, immunohistochemical studies on the cytoskeletal markers of the saurian glial cells are referred to *Anolis carolinensis* (limited to the cerebellum, Dahl et al. 1985), *Lacerta lepida* (Bodega et al. 1990, 1994), *Gallotia galloti* (Monzon-Mayor et al. 1990, 1998; Yanes et al. 1990), and *Lacerta sicula* (Lauro et al. 1991; Lazzari and Franceschini 2001).

Eublepharis macularius is a saurian belonging to the Gekkonidae family, particularly to the Eublepharinae subfamily, i.e. geckos provided with eyelids (according to other classifications this subfamily should be upgraded to the family, Eublepharidae). Eublepharinae, having mobile eyelids and lacking toe pads, are regarded to be primitive compared to the other gecko subfamilies (Gekkoninae, Diplodactylinae, Sphaerodactylinae).

The aim of the present work is to extend the knowledge about the glial cytoarchitecture in saurians with regard to brain evolution, by studying the glia in the leopard gecko, *E. macularius*, through the immunohistochemical detection of GFAP and vimentin which are molecular markers specific for the glial intermediate filaments.

Materials and methods

Six adult leopard geckos, *E. macularius* (Blyth 1854; 15–20 cm total length) of both sexes, were obtained from the "Acquario Fossolo", Bologna, Italy. These lizards were kept in terraria at room temperature in a natural light–dark cycle and fed ad libitum with living insects. All procedures were in conformity with the guidelines of the European Communities Council Directive (86/609/CEE), the current Italian legislation for the use and care of animals, and the guidelines of the U.S. National Institute of Health. This study was also approved by the Ethic-Scientific Committee of the University of Bologna.

After a deep anesthesia with ethyl ether, the brains and spinal cords were rapidly dissected and fixed by immersion in a modified Bouin fixative consisting of saturated aqueous solution of picric acid and formalin (ratio 3:1) for 6 h at 4°C. The picric acid was removed by long washing in 50% aqueous solution of ethanol, then the specimens were dehydrated in a graded series of ethanol and embedded in Paraplast plus (Sherwood Medical, St. Louis, MO, USA; melting point 55–57°C). Transverse sections (8 μm in thickness) were set on poly-L-lysine (Sigma, St. Louis, MO, USA) coated slides. In the following treatment, all washing and incubation solutions, with the exception of those containing primary antibodies, were employed at room temperature. The sections were deparaffinized with xylene, hydrated, and pretreated for 20 min with 1% H_2O_2 in 0.05 M phosphate buffer solution (PBS) with 0.15 M NaCl , pH 7.4, in order to quench endogenous peroxidase activity. Afterward they were pre-incubated in PBS containing 10% normal goat serum (NGS; Vector, Burlingame, CA, USA), 1% bovine serum albumine (BSA; Sigma) and 0.1% Tween 20 (Merck, Darmstadt, Germany) for 30 min to reduce non-specific background staining. After the H_2O_2 treatment, the sections for vimentin immunostaining were also treated for 15 min in PBS containing 0.1% pronase (Merck) as the antigen unmasking step. The sections were incubated overnight in a moist chamber on a floating plate in either a rabbit polyclonal anti-cow GFAP antiserum (1:500; Dakocytomation, Glostrup, Denmark) or a mouse monoclonal anti-bovine vimentin antibody (1:5; Cymbus Biotechnology, Chandlers Ford, UK). The antibodies were diluted in PBS containing 3% NGS, 1% BSA, 0.1% Tween 20, and 0.02% sodium azide. After washing in PBS with 0.1% Tween 20 (three times, 8 min each), the sections were incubated in the secondary antibodies for 2 h: HRP-conjugated goat anti-rabbit IgG (1:200; Vector) for GFAP- and HRP-conjugated goat anti-mouse IgG (1:100, Vector) for vimentin. After rinsing in 0.1% Tween 20 in PBS, the sections were immersed in 0.1 M PBS, pH 7.4, for 10 min and treated with the diaminobenzidine method (DAB) modified by Adams (1981). The sections were then dehydrated in ethanol, cleared in xylene and coverslipped with Permount (Fisher Scientific, Pittsburgh, PA, USA). The negative controls were obtained by omission of the primary antibodies, replaced by 3% NGS.

Results

GFAP-like immunoreactivity

In the leopard gecko, GFAP-immunostained elements could be observed throughout the CNS in both the gray and the white matters. The general pattern of GFAP-immunopositivity consisted of long fibers originating from cell bodies located in the ependymal layer

(Fig. 1a). The apical poles of these cells delimited the surface of the ventriculi. The abluminal regions gave rise to fibers that ran parallel to each other and have a radial arrangement through the neural wall. These fibers ended perpendicularly to the pial surface where they formed variously extended end-feet constituting the submeningeal glial layer (Fig. 1b). The proximal tract, next to the ventricular wall, and the distal one, next to the meningeal surface, were generally thicker than the intermediate segment. Thus these cells appeared to have a tanycytic character. In every region of the CNS, thin immunopositive fibers reached the outer side of the vascular walls where they formed adjacent end-feet, which formed the perivascular glial coating (Fig. 1c). The radial ependymoglia showed regional specialization in relation to the different size and immunocytochemical staining intensities of their cell bodies and cytoplasmatic processes. But, light microscopy immunohistochemistry of intermediate filament markers could not show the whole extension of the glial cells as it stained only the cell regions, which contained immunoreactive fibers.

The GFAP-immunopositive star-shaped astrocytes were seen in several brain areas. They have round cell bodies giving rise to short branched processes (Fig. 1d). Star-shaped astrocytes (proper astrocytes) were not the main immunopositive structures in any nervous area, but were always mixed with predominant long radial fibers.

The characteristics of the GFAP-immunopositive pattern in the different areas of the CNS is described in the following paragraphs.

In the olfactory bulb, the ependymal cells showed elliptical cell bodies orthogonally placed to the ventricular cavity (Fig. 2a). Three layers could be schematically detected. In the gray matter (internal granular layer), next to the ependyma, the glial fibers appeared straight and clearly radially oriented. They became irregularly arranged in the intermediate layer (molecular layer). A greater degree of irregularity appeared in the outer zone, corresponding to the glomerular and external plexiform layers, where the fibers intertwined while approaching the meningeal surface.

In the olfactory peduncles, the narrow internal cavity was clearly lined by a GFAP-immunopositive ependyma (Fig. 2b). It gave rise to radial glial fibers, which were bent, in the central part of the median zone and orthogonally oriented to the meningeal surface in their terminal course. In the lateral and ventral marginal zones of the peduncles, the glial fibers gave rise to densely woven glial structures.

In the telencephalic cortex, the neural wall appeared thin and the immunostaining schematically revealed three layers (Fig. 2c, d): a deep periependymal zone with thick radial glial fibers rather regularly oriented, a middle zone in which the fibers were less evident and somewhat irregularly oriented due to the presence of

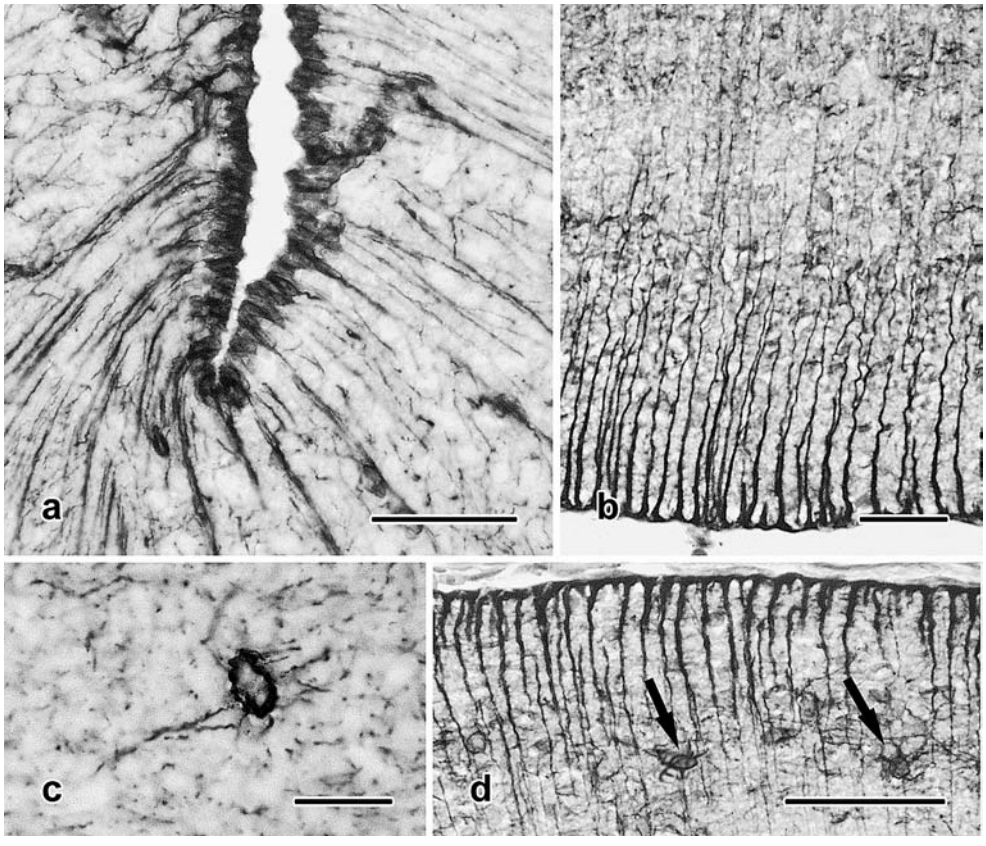

Fig. 1 GFAP immunohistochemical staining pattern in the CNS of *Eublepharis macularius*. **a** Ependymal radial glial cells in the ventral sulcus of the telencephalon. **b** The end-feet of radial fibers form the submeningeal glial layer in the lateral tegmentum of the mesencephalon. **c** Perivascular glial layer surrounds a telencephalic vessel. **d** Star-shaped astrocytes (*arrows*) are present in the superficial layer of the mesencephalic optic tectum among the radial processes. Scale bars = 50 μm (**a**, **d**), 100 μm (**b**), 25 μm (**c**)

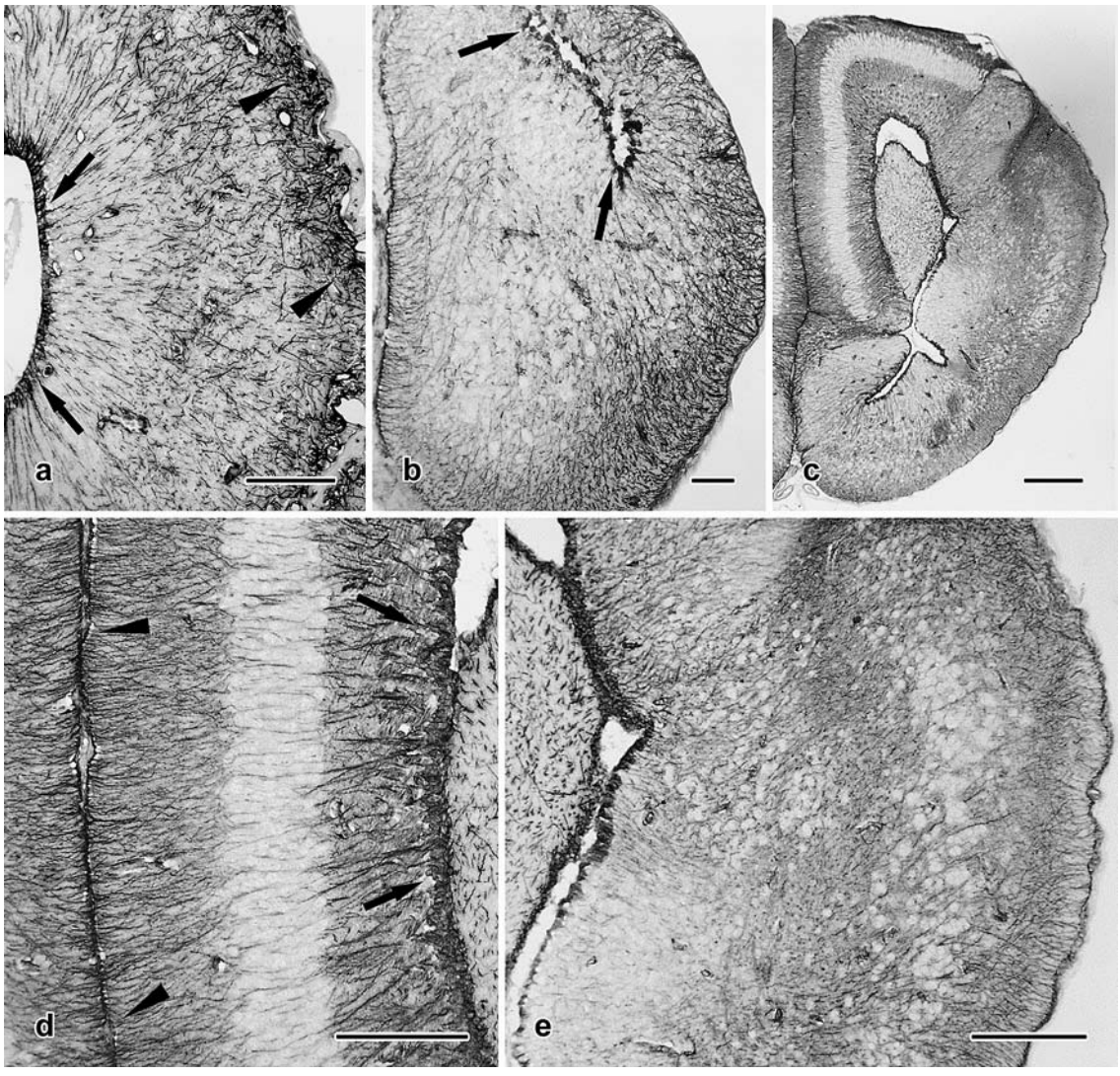

Fig. 2 GFAP-immunostaining of the astroglia in the telencephalon of *Eublepharis macularius*. **a** Distribution of immunopositive structures in the olfactory bulb (*arrows* ependyma, *arrowheads* meningeal surface). **b** GFAP-immunopositive elements in the olfactory peduncle (*arrows* ependyma). **c** GFAP-immunopositivity in the telencephalon. **d** Three zones of radial glial processes in the telencephalic cortex (*arrows* ependyma, *arrowheads* meningeal surface). **e** The radial arrangement of the glial processes is less evident in the striatum. Scale bars = 100 μm (**a**, **b**, **d**, **e**), 200 μm (**c**)

large neurons, and a superficial (submeningeal) zone where thin immunostained glial fibers reached the submeningeal surface with a slight weavy coarse. This arrangement became less evident in the telencephalic regions showing increased thickness of the neural wall (septum, striatum, and dorsal ventricular ridge) (Fig. 2c, e). In the telencephalon, star-shaped astrocytes were not found. In the middle part of the telencephalon, the three-layered pattern of the cortex was clearly limited only to the medial and dorsomedial cortexes (Fig. 3a, b), and the septum was crossed by evident fibers originating from the median zone of the septal ependyma. They were ventrally curved and converged toward the anterior commissure (Fig. 3c). Evident radial fibers emerged from the striatum ependyma and bent toward the ventrolateral meningeal surface (Fig. 3d). In the ventral sulcus, the ependymal cells were somewhat larger and more stained (Fig. 1a).

In the anterior part of the diencephalon, the narrow third ventricle was clearly stained by an immunopositive ependyma. In the central part of the diencephalon, the glial fiber immunostaining appeared more evident in the habenular region and in the lateral thalamus (Fig. 3e). The optic tract was clearly immunopositive with fibers parallel to the axons (Fig. 3e). The ependymal cells gave rise to positive glial fibers that appeared orthogonally oriented to the ventricular surface in their proximal tract, and then became thinner and less evident (Fig. 3f). In the epithalamic region, these fibers appeared curving laterodorsally toward the habenular nuclei (Fig. 3g). In the hypothalamic region, the radial fibers showed an arched course from the floor of the third ventricle to the

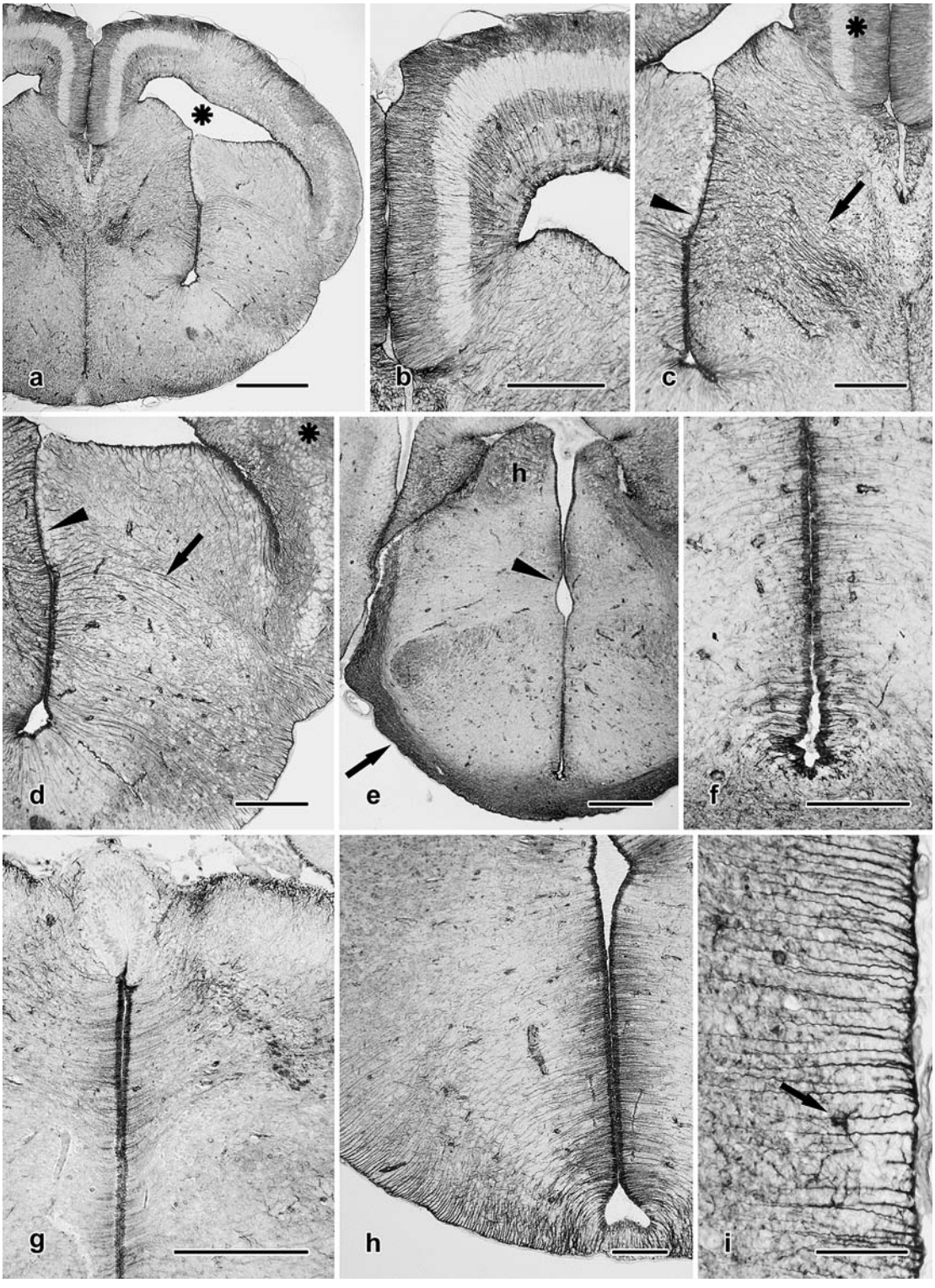

Fig. 3 GFAP-immunostaining in the telencephalon and mesencephalon of *Eublepharis macularius*. **a** Distribution of immunopositivity in the posterior part of the telencephalon and in the anterior part of the diencephalon (*asterisk* fourth ventricle). **b** Radial glial processes in the medial and dorsal cortex of the telencephalon. **c** Immunopositive fibers in the septum (*arrow*) (*arrowhead* ventral sulcus of the ventriculum, *asterisk* medial cortex of the telencephalon). **d** *Arrow* indicates radial glial elements in the striatum (*arrowhead* ventral sulcus of the ventriculum, *asterisk* lateral cortex of the telencephalon). **e** Distribution of GFAP-immunopositivity in the middle part of the diencephalon (*arrow* optic tracts, *h* habenula, *arrowhead* the third ventricle). **f** Ependymal radial glia in the ventral part of diencephalic ventricle. **g** Ependymal radial glia in the dorsal part of the diencephalic ventricle. **h** Immunopositive elements in the hypothalamic region in the posterior diencephalon. **i** A star-shaped astrocyte (*arrow*) in the superficial zone of the lateral diencephalon. Scale bars = 400 μm (**a**, **e**), 200 μm (**b**–**d**, **g**), 100 μm (**f**, **h**), 50 μm (**i**)

meningeal surface (Fig. 3h). Regularly arranged radial glial fibers were clearly immunopositive at the submeningeal level of the lateral and ventral parts of the diencephalon. A few star-shaped astrocytes were detected in the ventral and lateral region of the diencephalon in the layer containing clear radial fibers approaching the meningeal surface (Fig. 3i).

In the mesencephalon, the ependyma was intensely GFAP-immunopositive (Fig. 4a). In the optic tectum, it gave rise to thin fibers, faintly stained, which crossed the tectal layers and became thicker and more heavily immunostained in the submeningeal layer (Fig. 4b). In this superficial layer, few GFAP-immunopositive star-shaped astrocytes were found (Fig. 4c). Thin radial fibers were observed in the torus semicircularis (Fig. 4d). In the anterior and posterior mesencephalon, where the ventriculum was reduced to a narrow cross-like shaped channel, all the four corners showed "ponytail" bundles of GFAP-immunopositive glial fibers (Fig. 4e, f). Radial fibers were observed in the submeningeal layer of the tegmentum that in the latero-ventral zone contained a few star-shaped astrocytes (Fig. 4g). They generally had rounded cell bodies and very short cytoplasmic processes. In the lateral tegmentum, under the layer of well-defined submeningeal radial elements, thick fibers were detected parallel to the meningeal surface (Fig. 4h).

In the cerebellum, the ependyma lining the dorsal cover of the fourth ventricle was GFAP-immunonegative (Fig. 5a). In the ventral zone of the granular layer, just dorsally to the fourth ventricle, radial immunopositive fibers were visible only in the midline. In the dorsal and lateral sides of the cerebellum, the granular stratum was covered by a slight submeningeal end-feet layer originating from radial fibers that were more evident and regularly arranged only in the peripheral zone (Fig. 5b). The molecular and granular layers were separated by an irregular layer containing GFAP-immunonegative areas corresponding to the positions of the Purkinje cells. All over the molecular layer, thin immunopositive fibers were transversely or obliquely cut (Fig. 5b).

In the medulla oblongata, the ependymal layer is clearly GFAP-immunopositive and gave rise to "ponytail" bundles of GFAP-immunopositive fibers at the level of the middle and lateral sulci (Fig. 5a, c). Some thin fibers extended from the median bundle along the raphe (Fig. 5d). The medial longitudinal fasicle was not circumscribed nor subdivided by immunopositive fibers. GFAP-immunopositive fibers were observed in the submeningeal layer of the lateral and ventral zones of the medulla oblongata where they formed the superficial glial layer with their end-feet (Fig. 5d, e). In this submeningeal layer near the medullar midline, a few star-shaped astrocytes were detected.

In the spinal cord, the GFAP-immunopositivity was intensely expressed in the white matter, more reduced in the gray substance, except in the periependymal zone (Fig. 6a, b). The ependyma was immunonegative but in the central zone of the gray matter, radial astrocyte cell bodies were displaced from the ependymal layer into the periependymal position. These immunopositive astrocytes with their processes circumscribed the ependymal canal and the medial longitudinal fasicles (Fig. 6b). The radial astrocytes located ventrally to the ependymal canal sent their processes along the midline to the ventral septum of the spinal cord. Star-shaped astrocytes were found in the lateral columns of the white matter and ventrally at the boundary between the white and the gray matters (Fig. 6b, c).

In control sections, no specific immunoreaction was found after incubation in the medium in which the primary anti-GFAP antibody was replaced by NGS.

Vimentin-like immunoreactivity

The olfactory bulb and peduncles did not show vimentin-immunopositivity associated to glial structures (Fig. 6d). In the median part of the telencephalon, vimentin-immunopositive glial elements were observed in the medial cortex and in the ventral part of the septum (nucleus accumbens) (Fig. 6e). In the medial cortex, they were represented by radial fibers approaching the meningeal surface and by some radial fibers in the periependymal layer at the dorsal corner of the telencephalic ventricle (Fig. 6f). In the nucleus accumbens, the stained fibers partly converged toward the medial meningeal surface, and partly were ventrally directed and less stained (Fig. 6g).

In the diencephalon, a clear vimentin-immunopositivity appeared in the optic tracts and nerves where the stained fibers were parallel to the axons (Fig. 6h). Immunopositive ependymal radial glial cells were found in the ventral part of the fourth ventricle (Fig. 6i).

In the mesencephalon, where the ventricular cavity was reduced to a cross-shaped canal, the ependyma of the dorsal corner showed immunopositivity (Fig. 6j). Immunopositive glial structures were not found in the other parts of the mesencephalon, cerebellum, and medulla oblongata.

In the spinal cord, vimentin-immunopositivity was associated to glial fibers on the midline (Fig. 6k). They originated from unstained cell bodies and were located diametrically opposed in the periependymal position on the dorsal and ventral sides of the ependymal layer (Fig. 6l). The dorsal fibers gave rise to a thick stained fasicle that extended to the dorsal septum. On the ventral side of the ependymal canal, the vimentin-immunopositive elements were observed extending for a shorter distance between the medial longitudinal fasicles.

In the CNS of the leopard gecko, a clear vimentin-immunopositivity was shown by erythrocytes still present in the vessels of the neural walls (Fig. 6m).

No staining was detected in the control sections containing NGS instead of the primary anti-vimentin antibody.

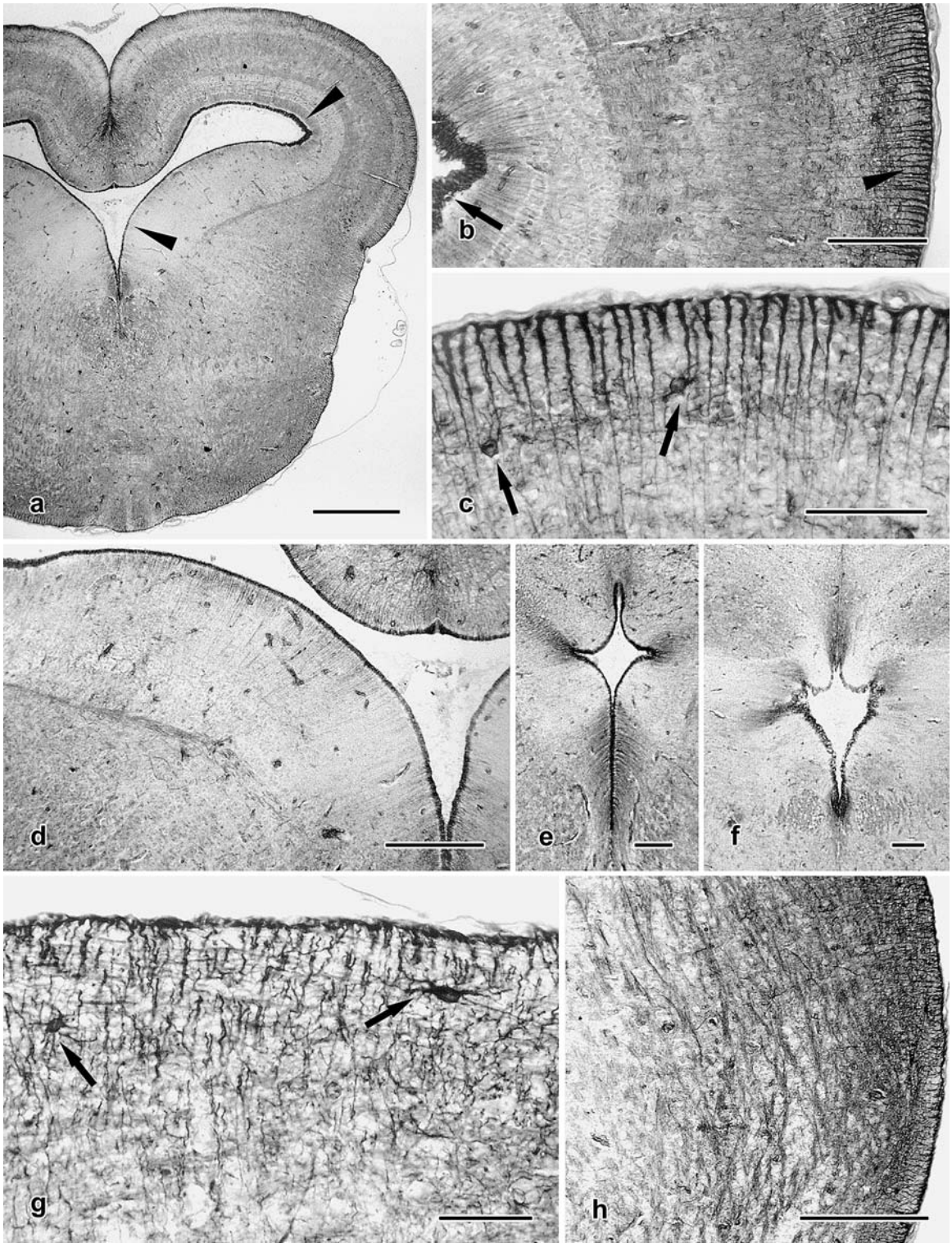

Fig. 4 GFAP-immunostaining in the mesencephalon of *Eublepharis macularius*. **a** The mesencephalic ependyma is clearly immunopositive (*arrowheads*). **b** Radial glial structures in the optic tectum (*arrow* ependyma, *arrowhead* meningeal surface). **c** Radial glial processes form the submeningeal glial layer. Star-shaped astrocytes (*arrows*) are present. **d** Glial fibers in the torus semicircularis. **e** Immunopositive radial glial elements outline the cross-shaped ependymal channel in the anterior part of the mesencephalon. **f** Immunopositive structures associated with the cross-shaped ependymal channel in the posterior part of the mesencephalon. **g** Star-shaped astrocytes (*arrows*) in the submeningeal zone of the ventral tegmentum. **h** Thick immunopositive fibers in the lateral tegmentum. Scale bars = 400 μm (**a**), 100 μm (**b**, **e**, **f**), 50 μm (**c**, **g**), 200 μm (**d**, **h**)

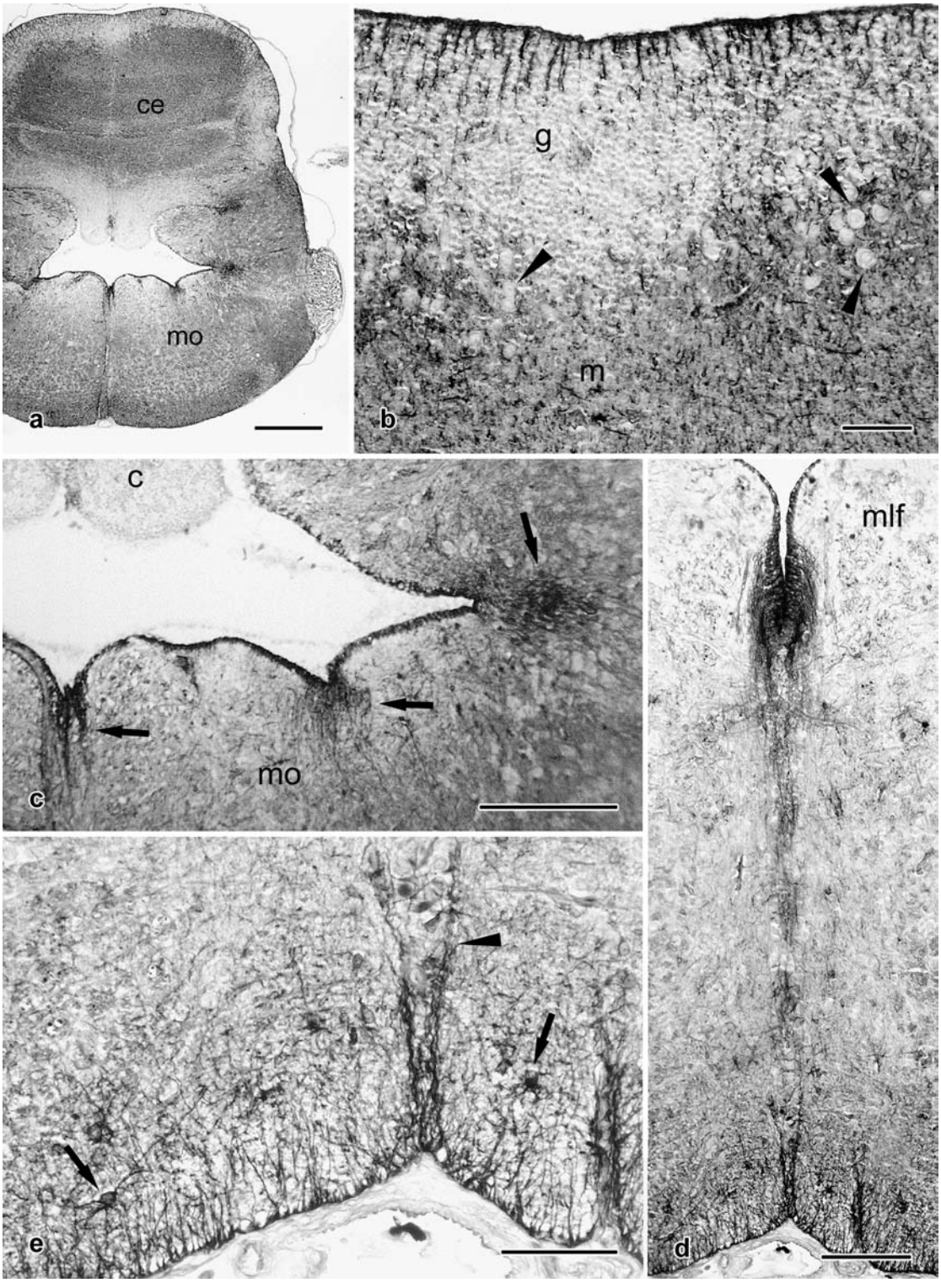

Fig. 5 GFAP-immunostaining in the cerebellum and medulla oblongata of *Eublepharis macularius*. **a** Distribution of GFAP-immunopositivity in the cerebellum (*ce*) and in the medulla oblongata (*mo*). The ependyma of the cerebellum is GFAP-immunonegative. **b** Distribution of immunopositivity in the dorsal zone of the cerebellum (*m* molecular layer, *g* granular layer, *arrowheads* Purkinje cells). **c** Ependymal radial glia at the level of the fourth ventricle. Bundles of stained fibers are present at the sulci level (*arrows*) (*c* cerebellum, *mo* medulla oblongata). **d** Immunopositive glial elements extending along the raphe (*mlf* medial longitudinal fasicle). **e** Star-shaped astrocytes (*arrows*) in the submeningeal layer of the ventral region of the medulla oblongata (*arrowhead* raphe). Scale bars = 400 μm (**a**), 50 μm (**b**, **e**), 200 μm (**c**), 100 μm (**d**)

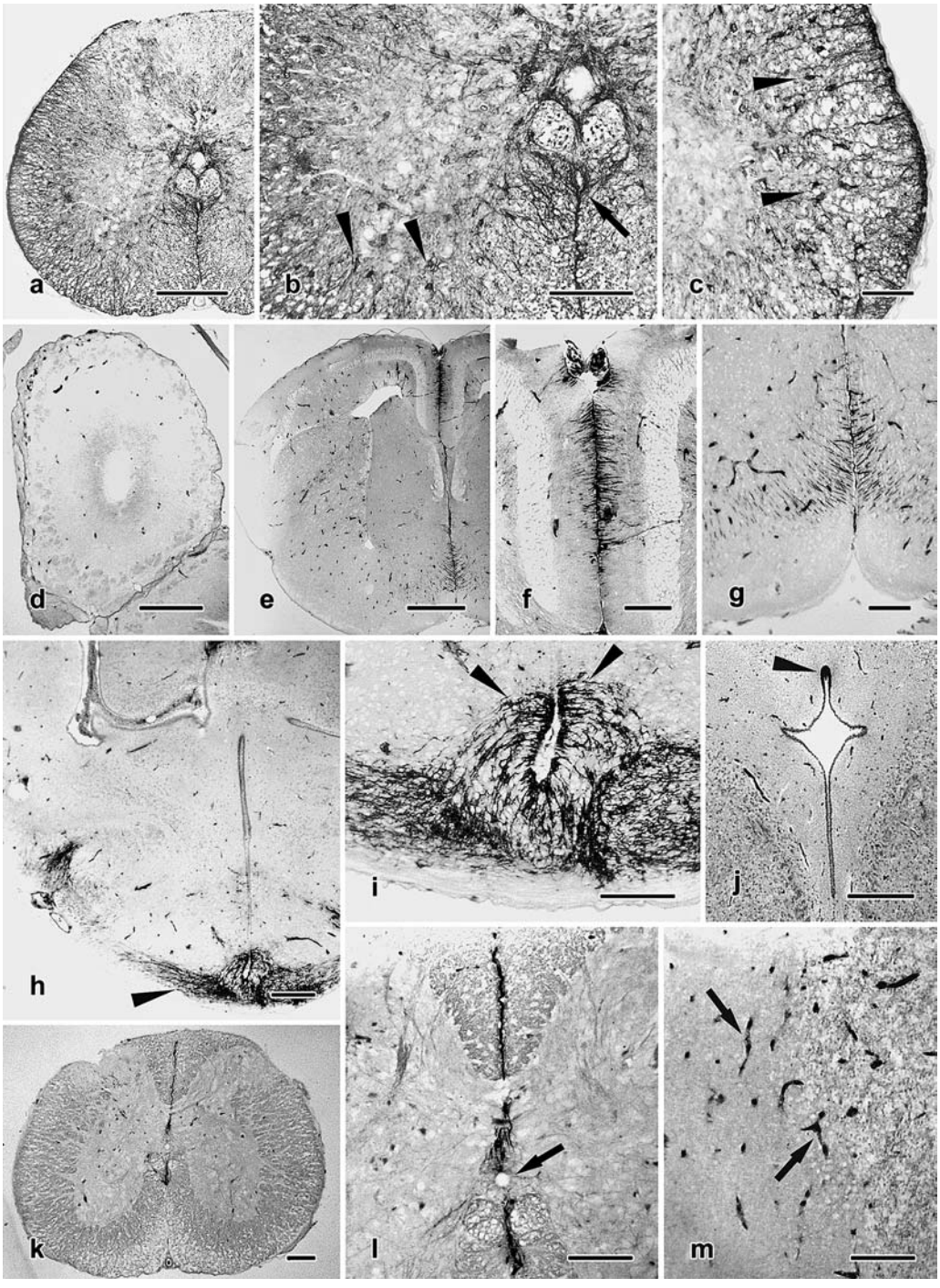

Fig. 6 GFAP-immunostaining in the spinal cord (**a**–**c**) and vimentin- immunostaining in the CNS (**d**–**m**) of *Eublepharis macularius*. **a** GFAP- immunopositive structures in the gray and white matters of the spinal cord. **b** Immunopositive radial elements in the central region of the spinal cord. Star- shaped astrocytes are located in the ventral horns (*arrowheads*) (*arrow* ependymal channel). **c** Astrocytes (*arrowheads*) in the lateral column of the spinal cord. **d** The olfactory bulb do not show vimentin-immunopositive glial structures. **e** In the telencephalon, vimentin-immunopositive glial elements are located in the middle line. **f** Vimentin-immunopositive glial structure in the medial cortex of the telencephalon. **g** Vimentin-immunopositive fibers in the region of nucleus accumbens. **h** In the diencephalon, the optic tract is vimentin-immunopositive (*arrowhead*). **i** Vimentin-immunopositive ependymal radial glia (*arrowheads*) are stained in the ventral part of the fourth ventricle. **j** In the mesencephalon, the cross-shaped channel shows vimentin-immunopositivity associated with the dorsal corner (*arrowhead*). **k** Vimentin-immunopositivity in the spinal cord. **l** In the spinal cord vimentin-positive elements are located in the middle line, dorsally and ventrally to the ependymal channel (*arrow*). **m** The erythrocytes inside the vessels show clear vimentin-immunopositivity (*arrows*). Scale bars = 200 μm (**a**, **d**, **h**, **j**), 100 μm (**b**, **f**, **g**, **i**, **k**–**m**), 50 μm (**c**), 400 μm (**e**)

Discussion

This immunohistochemical study points out the presence of different astroglial cell types in the CNS of *E. macularius*. Moreover, in the different nervous regions, the staining intensity appears not to be identical even in the same cellular type. These observations result in a heterogeneous feature of the astroglial pattern in *E. macularius*, comparable with *G. galloti* (Monzon-Mayor et al. 1990, 1998) and *Podarcis sicula* (Lazzari and Franceschini 2001). The regional variability of the glial pattern in *E. macularius* is significantly greater than in anurans (Lazzari et al. 1997) and dipnoi (Lazzari and Franceschini 2004), but reduced compared to the caiman (Kalman and Pritz 2001) and greatly less evident than in chicken (Kalman et al. 1993, 1998). This may suggest that different brain regions need different glial functions and the glial pattern fits the requirements of the different nervous areas.

The glial cytoarchitecture changes in the developing mammals: in fact, the radial glia which are shown prenatally, disappear postnatally (Voight 1989; Elmquist et al. 1994), whereas in the other vertebrates, radial glial elements are still retained in adults (urodels, Zamora and Mutin 1988; Lazzari et al. 1997; reptiles, Monzon-Mayor et al. 1990; Yanes et al. 1990; Kalman et al. 1994; Lazzari and Franceschini 2001; birds, Kalman et al. 1993). The development is also characterized by a change in the molecular composition of the glial intermediate filaments. In mammals, vimentin is progressively replaced by GFAP as the development proceeds (Oudega and Marani 1991; Elmquist et al. 1994). This developmental vimentin-GFAP shift has also been reported in reptiles (Monzon-Mayor et al. 1990; Yanes et al. 1990) and in birds (Tapscot et al. 1981; Kalman et al. 1998), however this shift is not complete. In fact, vimentin-immunopositive glial elements are still found in adult teleosts (Cardone and Roots 1990; Rubio et al. 1992; Bodega et al. 1993), urodels (Zamora and Mutin 1988; Lauro et al. 1991; Lazzari et al. 1997), birds (Alvarez-Buylla et al. 1987; Kalman et al. 1998), and mammals (Chouaf et al. 1989; Oudega and Marani 1991; Yamada et al. 1992). In adult reptiles, vimentin-immunopositive glial elements have been reported in the tegmentum of *G. galloti* (Monzon-Mayor et al. 1990) and in the ventral diencephalon and in the spinal cord of *P. sicula* (Lazzari and Franceschini 2001). No vimentin-immunopositive glial strucures were found in *Anolis sagrei* (Lazzari and Franceschini 2005), therefore this reptile appears to have completed the shift from vimentin to GFAP expression in the intermediate filaments of its astroglial cells. This transition in protein expression has not been completed in *E. macularius*. Moreover its moderate vimentin-immunopositivity, greater than in other saurians, supports a more immature condition. Immunohistochemical studies on the co-localization of GFAP and vimentin in the CNS of reptiles are not available yet. They may show the astrocyte populations, which either express one or both of the epitopes and may add more detailed information.

The presence and distribution of true astrocytes, usually named star-shaped astrocytes, represent another problem in the glial cytoarchitecture. The absence of GFAP-immunopositive star-shaped astrocytes in the telencephalon of *E. macularius* is in accordance with the observations in *G. galloti* (Yanes et al. 1990) and *P. sicula* (Lazzari and Franceschini 2001) whose telencephalons show only GFAP-positive radial glia. On the contrary, some true astrocytes are found in the telencephalon of *A. sagrei* (Lazzari and Franceschini 2005). As regards the other reptiles, the turtle telencephalon lacks star-shaped astrocytes and its CNS has only a radial glial pattern (Kalman et al. 1994). On the contrary, the snake hippocampus expressed GFAP-immunopositive star-shaped astrocytes (Onteniente et al. 1983). Therefore, the telencephalic glial cytorchitecture seems more advanced in those reptiles, which contain star-shaped astrocytes, even if scarce. Radial astrocytes and star-shaped ones coexist in the mesencephalon of *A. sagrei* (Lazzari and Franceschini 2005), *G. galloti* (Monzon-Mayor et al. 1990, 1998), *P. sicula* (Lazzari and Franceschini 2001), and *E. macularius* (present study). Whereas *G. galloti* and *P. sicula* show star-shaped astrocytes only in the optic tectum, both *A. sagrei* and *E. macularius* possess scarce true astrocytes in the ventral and ventrolateral regions of mesencephalon (tegmentum) and medulla oblongata. Furthermore, while in the optic tectum of *P. sicula*, the star-shaped astrocytes are numerous and mainly disposed in two layers (Lazzari and Franceschini 2001); in the optic tectum of *A. sagrei* as well as that of *E. macularius*, they are in smaller number and arranged in only one layer.

The results reported in the present study can be explained assuming that in these lizards, the glial cytoarchitecture of the telencephalon is more primitive than the mesencephalic one. Moreover, the astroglial pattern in the optic tectum of *P. sicula* is more complex and evolved than in *G. galloti*, *A. sagrei* and *E. macularius*. These studies emphasize a degree of heterogeneity in the glial architecture of saurians, even if further comparative studies are needed in representatives from other families, genera, and species to confirm this idea.

Compared with radial elements, the star-shaped astrocytes are considered more advanced in evolution, constituting a more variable glial network which sustains neural wall thickening and different GFAP expression in the brain regions as adaptation to the requirements of the regional neuronal environment (Kalman and Pritz 2001).

Radial glial cells are involved in neuronal migration during the development of the CNS. Their persistence in the adult non-mammalian vertebrates could be associated with the retention of a certain degree of neuronal plasticity even in the adult state. But, in addition to phylogenetic and ontogenetic trends, species-specific functional consequences might be responsible for some

aspects of the glial cytoarchitecture. There are no such functional aspects known yet, so further research related to possible functional characteristics is needed in order to achieve a comprehensive understanding of the different types of glia.

In the spinal cord of *E. macularius*, the ependymal GFAP- and vimentin- immunonegativity is in accordance with the condition of *A. sagrei* (Lazzari and Franceschini 2005) and *L. lepida* (Bodega et al. 1994), but it differs from *P. sicula* which shows clear vimentin-immunopositivity (Lazzari and Franceschini 2001). Technical differences rather than species-related differences could be considered in the interpretation of these different immunostaining results.

In the white matter of the mammalian spinal cord, the GFAP-immunostaining of the fibrous astrocytes is more intense compared to the gray matter (Dahl and Bignami 1985). This tendency is already found in *P. sicula* (Lazzari and Franceschini 2001) but is reduced in both *E. macularius* (present study) and *A. sagrei* (Lazzari and Franceschini 2005) characterized by less star-shaped astrocytes showing smaller cell bodies and reduced processes.

The glial cytoarchitecture of *E. macularius* is characterized by a radial glial system prevailing over the star-shaped astrocytes, which are not regularly arranged. The GFAP-immunostaining in *E. macularius* shows slight differences which, according to Kalman (1998) may be referred to an uneven distribution as well as to a different size of the astroglial elements rather than to differential GFAP expression as reported in birds and mammals. From the present study in *E. macularius*, the glial cytoarchitecture in saurians appears composed of the basic radial glial system, but differences are found in the number and location of the star-shaped astrocytes. These differences could be related to slight diversities in the glial maturation process that is clearly observed in reptiles. The glial pattern of *E. macularius* is comparable to what is found in *A. sagrei* (Lazzari and Franceschini 2005) but more complex than in urodeles (Lazzari et al. 1997) and in *Protopterus annectens* (Lazzari and Franceschini 2004). It is also slightly simpler than in *P. sicula* (Lazzari and Franceschini 2001) and clearly less elaborate than in teleosts (Kalman 1998), birds, and mammals (Kalman et al. 1993; Elmquist et al. 1994).

This study strongly supports that reptiles are an important step in the evolution of vertebrate glia.

Acknowledgements This work was supported by grants from the Italian Ministero dell'Istruzione, dell'Università e della Ricerca.

References

Adams JC (1981) Heavy-metal intensification of DAB-based reaction product. J Histochem Cytochem 29:775

Alvarez-Buylla A, Buskirk DR, Nottebohm F (1987) Monoclonal antibody reveals radial glia in adult avian brain. J Comp Neurol 264:159–170

Bennett GS, Fellini SA, Holtzer H (1978) Immunofluorescent visualization of 100 A filaments in different cultured chick embryo cell types. Differentiation 12:71–82

Bodega G, Suarez I, Rubio M, Fernandez B (1990) Distribution and characteristics of the different astroglial cell types in the adult lizard (*Lacerta lepida*) spinal cord. Anat Embryol 181:567–575

Bodega G, Suarez I, Rubio M, Villaba RM, Fernandez B (1993) Astroglial pattern in the spinal cord of the adult barbel (*Barbus comiza*). Anat Embryol 187:385–395

Bodega G, Suárez I, Rubio M, Fernández B (1994) Ependyma: phylogenetic evolution of glial fibrillary acidic protein (GFAP) and vimentin expression in vertebrate spinal cord. Histochemistry 102:113–122

Cardone B, Roots BJ (1990) Comparative immunohistochemical study of glial filament proteins (glial fibrillary acidic protein and vimentin) in goldfish, octopus and snail. Glia 3:180–192

Chouaf L, Didier-Bazes M, Aguera M, Tardy M, Sallanon M, Kitahama K, Belin MF (1989) Comparative marker analysis of the ependymocytes in the subcommissural organ in four different mammalian species. Cell Tissue Res 257:255–262

Dahl D, Bignami A (1973) Immunochemical and immunofluorescence studies of the GFAP in vertebrates. Brain Res 61:279–293

Dahl D, Bignami A (1985) Intermediate filaments in nervous tissue. In: Shay JW (ed) Cell and muscle motility, vol 6. Plenum Press New York, pp 75–96

Dahl D, Crosby CJ, Sethi JS, Bignami A (1985) Glial fibrillary acidic (GFA) protein in vertebrates: immunofluorescence and immunoblotting study with monoclonal and polyclonal antibodies. J Comp Neurol 239:75–88

Ebner FF, Colonnier M (1975) Synaptic patterns in the visual cortex of turtle: an electron microscopic study. J Comp Neurol 160:51–80

Elmquist JK, Swanson JJ, Sakaguchi DS, Ross LR, Jacobson CD (1994) Developmental distribution of GFAP and vimentin in the Brazilian opossum brain. J Comp Neurol 344:283–296

Kalman M (1998) Astroglial architecture of the carp (*Cyprinus carpio*) brain as revealed by immunocytochemical staining against glial fibrillary acidic protein (GFAP). Anat Embryol 198:409–433

Kalman M, Pritz MB (2001) Glial fibrillary acidic protein-immunopositive structures in the brain of a crocodilian, *Caiman crocodilus*, and its bearing on the evolution of astroglia. J Comp Neurol 431:460–480

Kalman M, Szekely A, Csillag A (1993) Distribution of glial fibrillary acidic protein-immunopositive structures in the brain of the domestic chicken (*Gallus domesticus*). J Comp Neurol 330:221–237

Kalman M, Kiss A, Majorossy K (1994) Distribution of glial fibrillary acidic protein-immunopositive structures in the brain of the red-eared freshwater turtle (*Pseudemys scripta elegans*). Anat Embryol 189:421–434

Kalman M, Martin-Partido G, Hidalgo-Sanchez M, Majorossy K (1997) Distribution of glial fibrillary acidic protein–immunopositive structures in the developing brain of the turtle *Mauremys leprosa*. Anat Embryol 196:47–65

Kalman M, Szekely AD, Csillag A (1998) Distribution of glial fibrillary acidic protein and vimentin-immunopositive elements in the developing chicken brain from hatch to adulthood. Anat Embryol 198:213–235

Lauro GM, Fonti R, Margotta V (1991) Phylogenetic evolution of intermediate filament associated proteins in ependymal cells of several adult poikilotherm vertebrates. J Hirnforsch 32:257–261

Lazzari M, Franceschini V (2001) Glial fibrillary acidic protein and vimentin immunoreactivity of astroglial cells in the central nervous system of adult *Podarcis sicula* (Squamata, Lacertidae). J Anat 198:67–75

Lazzari M, Franceschini V (2004) Glial fibrillary acidic protein and vimentin immunoreactivity of astroglial cells in the central nervous system of the African lungfish, *Protopterus annectens* (Dipnoi: Lepidosirenidae). J Morphol 262:741–749

Lazzari M, Franceschini V (2005) Astroglial Cells in the Central Nervous System of the Brown Anole Lizard, Anolis sagrei, revealed by Intermediate Filament Immunohistochemistry. J Morphol 265:325–334

Lazzari M, Franceschini V, Ciani F (1997) Glial Fibrillary Acidic Protein and Vimentin in radial glia of *Ambystoma mexicanum* and *Triturus carnifex*: An immunocytochemical Study. J Brain Res 38:187–194

Levitt P, Rakic P (1980) Immunoperoxidase localization of glial fibrillary acidic protein in radial glial cells and astrocytes of the developing rhesus monkey brain. J Comp Neurol 193:815–840

Miller RH, Liuzzi FJ (1986) Regional specialization of the radial glial cells of the adult frog spinal cord. J Neurocytol 15: 187–196

Monzon-Mayor M, Yanes C, Ghandour MS, De Barry J, Gombos G (1990) GFAP and vimentin immunohistochemistry in the adult and developing midbrain of the lizard *Gallotia galloti*. J Comp Neurol 295:569–579

Monzon-Mayor M, Yanes C, De Barry J, Capdevilla-Carbonell C, Renau-Piqueras J, Tholey G, Gombos G (1998) Heterogeneous immunoreactivity in glial cells in the mesencephalon of a lizard: a double labelling immunohistochemical study. J Morphol 235:109–119

Naujoks-Manteuffel C, Meyer DL (1996) Glial fibrillary acidic protein in the brain of the caecilian *Typhlonectes natans* (Amphibia, Gymnophiona): an immunocytochemical study. Cell Tissue Res 283:51–58

Onteniente B, Kimura H, Maeda T (1983) Comparative study of the glial fibrillary acidic protein in vertebrates by PAP immunohistochemistry. J Comp Neurol 215:427–436

Oudega M, Marani E (1991) Expression of vimentin and glial fibrillary acidic protein in the developing rat spinal cord: an immunocytochemical study of the spinal cord glial system. J Anat 179:97–114

Pixley SK, De Vellis J (1984) Transition between immature radial glia and mature astrocytes studied with a monoclonal antibody to vimentin. Brain Res 317:201–209

Pulido-Caballero J, Jiménez-Sampedro F, Echevarría-Aza D, Martínez-Millán L (1994) Postnatal development of vimentin-positive cells in the rabbit superior colliculus. J Comp Neurol 343:102–112

Rubio M, Suarez I, Bodega G, Fernandez B (1992) Glial fibrillary acidic protein and vimentin immunohistochemistry in the posterior rhombencephalon of the Iberian barb (*Barbus comiza*). Neurosci Lett 134:203–206

Szaro BG, Gainer H (1988) Immunocytochemical identification of non-neuronal intermediate filament proteins in the developing *Xenopus laevis* nervous system. Dev Brain Res 43:207–224

Tapscott SJ, Bennett GS, Toyama Y, Kleinbart F, Holtzer H (1981) Intermediate filament protein in the developing chick spinal cord. Dev Biol 86:40–54

Voigt T (1989) Development of glial cells in the cerebral walls of ferrets: direct tracing of their transformation from radial glia into astrocytes. J Comp Neurol 289:74–88

Wasowicz M, Pierre J, Reperant J, Ward R, Vesselkin NP, Versaux-Botteri C (1994) Immunoreactivity to glial fibrillary acidic protein (GFAP) in the brain and spinal cord of the lamprey (*Lampetra fluviatilis*). J Brain Res 35:71–78

Wicht H, Derouiche A, Korf H-W (1994) An immunocytochemical investigation of glial morphology in the Pacific hagfish: radial and astrocyte-like glia have the same phylogenetic age. J Neurocytol 23:565–576

Yamada K, Watanabe M (2002) Cytodifferentiation of Bergmann glia and its retationship with Purkinje cells. Anat Sci Int 77:94–108

Yamada T, Kawamata T, Walker DG, Mcgeer PL (1992) Vimentin immunoreactivity in normal and pathological human brain tissue. Acta Neuropathol 84:157–162

Yanes C, Monzon-Mayor M, Ghandour MS, De Barry J, Gombos G (1990) Radial glia and astrocytes in developing and adult telencephalon of the lizard *Gallotia galloti* as revealed by immunohistochemistry with anti-GFAP and anti-vimentin antibodies. J Comp Neurol 295:559–568

Zamora AJ, Mutin M (1988) Vimentin and glial fibrillary acidic protein filaments in radial glia of the adult urodele spinal cord. Neuroscience 27:279–288